Molecular Cancer Research

EZH2 or HDAC1 Inhibition Reverses Multiple Myeloma–Induced Epigenetic Suppression of Osteoblast Differentiation

Juraj Adamik[1], Shunqian Jin[1], Quanhong Sun[1], Peng Zhang[1], Kurt R. Weiss[2], Judith L. Anderson[3], Rebecca Silbermann[3], G. David Roodman[3,4], and Deborah L. Galson[1,5]

Abstract

In multiple myeloma, osteolytic lesions rarely heal because of persistent suppressed osteoblast differentiation resulting in a high fracture risk. Herein, chromatin immunoprecipitation analyses reveal that multiple myeloma cells induce repressive epigenetic histone changes at the *Runx2* locus that prevent osteoblast differentiation. The most pronounced multiple myeloma–induced changes were at the *Runx2-P1* promoter, converting it from a poised bivalent state to a repressed state. Previously, it was observed that multiple myeloma induces the transcription repressor GFI1 in osteoblast precursors, which correlates with decreased *Runx2* expression, thus prompting detailed characterization of the multiple myeloma and TNFα-dependent GFI1 response element within the *Runx2-P1* promoter. Further analyses reveal that multiple myeloma–induced GFI1 binding to *Runx2* in osteoblast precursors and recruitment of the histone modifiers HDAC1, LSD1, and EZH2 is required to establish and maintain *Runx2* repression in osteogenic conditions. These GFI1-mediated repressive chromatin changes persist even after removal of multiple myeloma. Ectopic GFI1 is sufficient to bind to *Runx2*, recruit HDAC1 and EZH2, increase H3K27me3 on the gene, and prevent osteogenic induction of endogenous *Runx2* expression. *Gfi1* knockdown in MC4 cells blocked multiple myeloma–induced recruitment of HDAC1 and EZH2 to *Runx2*, acquisition of repressive chromatin architecture, and suppression of osteoblast differentiation. Importantly, inhibition of EZH2 or HDAC1 activity in pre-osteoblasts after multiple myeloma exposure *in vitro* or in osteoblast precursors from patients with multiple myeloma reversed the repressive chromatin architecture at *Runx2* and rescued osteoblast differentiation.

Implications: This study suggests that therapeutically targeting EZH2 or HDAC1 activity may reverse the profound multiple myeloma–induced osteoblast suppression and allow repair of the lytic lesions. *Mol Cancer Res; 15(4); 405–17. ©2017 AACR.*

Introduction

Multiple myeloma, a malignant plasma cell disorder, is the most frequent cancer to involve bone (1). More than 80% of patients with multiple myeloma develop bone lesions that can result in severe pain and frequent pathologic fractures (2), a major contributor to patient morbidity and mortality (3). Multiple myeloma bone disease is characterized by increased osteolytic bone destruction with little or no new bone formation due to persistent multiple myeloma–induced suppression of bone marrow stromal cell (BMSC) differentiation into bone-forming osteoblasts (4, 5). This results in lesions that rarely heal, even when patients are in long-term remission. Furthermore, BMSCs from patients with multiple myeloma (MM-BMSC) or mouse multiple myeloma models and healthy donor BMSC (HD-BMSC) and pre-osteoblast cell lines exposed to multiple myeloma cells in culture demonstrate decreased osteoblast differentiation even after removal of the multiple myeloma cells and extended culture (6). This protracted selective suppression of osteoblast differentiation suggests that multiple myeloma cells induce a persistent, cell-autonomous change in MM-BMSC. Multiple myeloma–derived TNFα, CCL3, IL3/activin A, Dickkopf1, sclerostin, TGFβ, HGF, and IL7, as well as direct contact, contribute to osteoblast suppression (4, 7), but the mechanisms responsible for the sustained cell-autonomous blockade of osteoblast differentiation in the MM-BMSC are not well understood. Multiple myeloma–altered BMSCs also support multiple myeloma cell adhesion, growth, and chemoresistance via increased levels of adhesion molecules, chemokines, and cytokines and express an altered RANKL (TNFSF11)/osteoprotegerin ratio to favor osteoclastogenesis (8–12).

[1]Department of Medicine, Division of Hematology-Oncology, University of Pittsburgh Cancer Institute, University of Pittsburgh School of Medicine, Pittsburgh, Pennsylvania. [2]Department of Orthopaedic Surgery, University of Pittsburgh Medical Center, Cancer Stem Cell Laboratory, University of Pittsburgh Cancer Institute, University of Pittsburgh School of Medicine, Pittsburgh, Pennsylvania. [3]Department of Medicine, Division of Hematology-Oncology, Indiana University, Indianapolis, Indiana. [4]Richard L. Roudebush VA Medical Center, Indianapolis, Indiana. [5]McGowan Institute for Regenerative Medicine, Pittsburgh, Pennsylvania.

Note: Supplementary data for this article are available at Molecular Cancer Research Online (http://mcr.aacrjournals.org/).

Current position of S. Jin: Department of Pharmaceutical Sciences, University of Pittsburgh School of Pharmacy, Pittsburgh, PA, USA.

Corresponding Authors: Deborah L. Galson, Hillman Cancer Center Research Pavilion, Suite 1.19b, 5117 Centre Avenue, Pittsburgh, PA 15213. Phone: 412-623-1112; Fax: 412-623-1415; E-mail: galson@pitt.edu; and G. David Roodman, Hematology-Oncology, Indiana University, School of Medicine, 980 West Walnut Street, Suite C312, Indianapolis, IN 46202. Phone: 317-278-6255; Fax: 317-274-0396; E-mail: groodman@iu.edu

doi: 10.1158/1541-7786.MCR-16-0242-T

Osteoblast differentiation requires upregulation and activation of the critical transcription factor RUNX2/CBFA1/AML3 (RUNX2; ref. 13). We (6), and others (14), have shown that RUNX2 activity in osteoblast precursors is inhibited in multiple myeloma, but the mechanism is unclear. Our previous studies of multiple myeloma–exposed BMSC revealed that *Runx2* gene repression was correlated with elevated expression of growth factor independence 1 (GFI1), a transcription repressor (6). We found that BMSCs isolated from *Gfi1*$^{-/-}$ mice were significantly resistant to multiple myeloma–induced suppression of *Runx2*. Furthermore, siRNA *Gfi1* knockdown in MM-BMSCs restored expression of *RUNX2* and osteoblast differentiation markers osteocalcin (*OCN, BGLAP)* and bone sialoprotein (*BSP, IBSP)*. These studies suggested that GFI1 could be a novel therapeutic target for multiple myeloma bone disease. However, therapeutic targeting of transcription factors is difficult and GFI1 is a large multifunctional protein with multiple modes of action.

GFI1, a 55-kDa zinc finger containing member of the Snail/Gfi1 transcription repressor family that includes GFI1b, SNAIL (SNAI1), SLUG (SNAI2), IA-1 (INSM1), and MLT1 (INSM2) (15, 16), has diverse biologic functions and mechanisms of action and regulates various aspects of normal and malignant hematopoiesis as well as inner ear development (17, 18). The 422-aa human (423-aa murine) GFI1 contains an N-terminal SNAG domain, an unstructured intermediate domain, and 6 C-terminal C2-H2 Zn finger domains, of which Zn fingers 3 to 5 are required for sequence-specific DNA binding to a recognition sequence containing the "AA(T/G)C" core motif (15, 19). GFI1 interacts with various chromatin modifiers to mediate epigenetic repression of target genes. The GFI1 SNAG domain is critical in recruiting lysine-specific demethylase 1 (LSD1, KDM1A) with the REST corepressor (CoREST, RCOR1) to target genes regulating hematopoiesis (20). GFI1 recruitment of histone methyltransferase G9a (EHMT2) and histone deacetylase 1 (HDAC1) through the intermediate domain represses the promoter of cell-cycle regulator *CDKN1A* (21). GFI1 can also repress gene expression independently of its DNA-binding capability, as shown by its binding to and cooperation with the POZ-ZF transcription factor MIZ-1 (ZBTB17) at the *CDKN1A* and *CDKN2B* gene promoters (11, 22). In addition, GFI1 binding to other transcription factors can interfere with their DNA binding or transactivation properties, thereby repressing their targets without GFI1 DNA binding. For instance, GFI1 can antagonize binding of RELA to its target genes in lipopolysaccharide-stimulated macrophages (23), as well as inhibit PU.1 (SPI1)-dependent gene transcription during granulocyte development (24). Conversely, GFI1 enhances STAT3-mediated gene transactivation by interacting with and sequestering a STAT3-negative regulator PIAS3 (25). GFI1 also regulates gene expression of the T-cell receptor CD45 (PTPRC) at the level of alternative splicing by interacting with the splicing factor U2AF26 (U2AFIL4) (26). Thus, further study was necessary to understand how GFI1 influenced *Runx2* expression.

In the current study, we determined whether multiple myeloma cells induce GFI1-mediated epigenetic changes in the chromatin architecture of the *Runx2* locus in osteoblast precursors. We identified the chromatin modifiers recruited by GFI1 and explored if inhibition of these enzymatic activities could induce reversal of the persistent suppression of BMSCs to osteogenic differentiation, making them potential actionable therapeutic targets to improve bone health in patients with multiple myeloma.

Materials and Methods

Reagents

Reagents used in this study can be found in Supplementary Methods.

Cells and co-culture

All cultures described below contained 10% FCS–1% penicillin/streptomycin. The pre-osteoblast murine cell line MC3T3-E1 subclone-4 (MC4) was obtained from Dr. Guozhi Xiao (27, 28) in 2009, and subclone-14 (MC14) was obtained from ATCC (CRL-2594) in 2014. Both were maintained in ascorbic acid–free αMEM proliferation media. Murine 5TGM1-GFP-TK (5TGM1) multiple myeloma cells (6) and human MM1.S-GFP cells (11) were maintained in RPMI-1640. Cell lines were authenticated by morphology, gene expression profile, and tumorigenic capacity (multiple myeloma cells). MC4 cells were grown to 90% confluency prior to co-culture. Direct 5TGM1-MC4 (10:1) co-cultures and indirect co-cultures of MM1.S cells in Transwells (10:1) with MC14 cells were carried out in 50:50 RPMI-1640/αMEM proliferation media. MM1.S in Transwells (Corning Inc., 3450) or 5TGM1 cells were carefully removed (FACS analysis demonstrated that $\leq$1% 5TGM1 cells remained). The MC4 and MC14 cells were isolated immediately or subjected to osteoblast differentiation first. Scrambled control (SHC002, Sigma) and mouse *Gfi1* shRNA (Sigma, TRCN0000096706, 5′-CCTCATCACTCATAGCAGAAA-3′) in pLKO.1-puro lentiviruses were generated by the UPCI lentivirus core facility and used to stably transduce (with polybrene) MC4 cells, which were selected and maintained using puromycin (2.5 μg/mL).

Human samples and primary BMSC cultures

Bone marrow aspirates and multiple myeloma bone resections were collected in heparin from 15 healthy donors and 29 patients with multiple myeloma. Human studies were approved by the University of Pittsburgh and Indiana University IRBs. Samples were collected from participants after obtaining written informed consent in accordance with the Declaration of Helsinki. Bone marrow mononuclear cells were separated by Ficoll-Hypaque density sedimentation and the nonadherent cells removed after overnight incubation in IMDM-10%FCS. The adherent cultures were then continued for 21 days with media changes every 4 days to obtain BMSCs. Subconfluent cells were detached with trypsin and replated (10^5 cells/10-cm dish) for use at passages 2 and 3.

Osteoblast differentiation, and alkaline phosphatase and alizarin red assays

Osteoblast differentiation media (αMEM supplemented with 50 μg/mL ascorbic acid and 10 mmol/L β-glycerophosphate; for human cells, 10 nmol/L dexamethasone was also added) were added to primary BMSCs or MC4 cells with or without prior multiple myeloma exposure; media were changed every 3 days. Mineralization at times indicated was assessed using alizarin red staining (6). The staining density quantitation was carried out using a ProteinSimple FluorChem M imaging system.

DNAs

Construction of the −974/+111 *mRunx2 P1* promoter-pGL4.10[luc2] reporters containing wild-type, Δ−37/−7, or the GFI1 site mutations (L mutant **GG**GCTT, R mutant AAGC**CC**, and LR mutant **GG**GC**CC**) and generation of the expression vectors encoding Myc-tagged mGFI1-1–423 aa, -1–380 aa, or -239–423 aa (in pCS2-MT) from mGFI1-wt-pCDNA3.1 are detailed in the Supplementary Methods. All constructs were verified by DNA sequencing.

Transfection of *Runx2 P1* promoter-Luc reporters and GFI1 constructs

The *mRunx2 P1* promoter-reporters and pRL-TK plasmids (Promega) were transfected into MC4 cells with Lipofectamine 2000, along with empty (EV) or wt mGFI1 expression vectors, or treated with TNFα as indicated in figure legends. Luc and *Renilla* activities were measured in supernatants from lysed cells (48 hours) using the Dual-Luciferase Reporter Assay System (Promega). The normalized (to *Renilla*) relative Luc activities for each reporter construct were calculated as a percentage of the activity of the −974/+111 *mRunx2*-pGL4.10[luc2]-wt cotransfected with EV. Transfections of Myc-mGFI1-wt and Myc-mGFI1-deletions into MC4 for endogenous *Runx2* mRNA and chromatin immunoprecipitation (ChIP) analyses were carried using FuGENE HD (E2311, Promega). See Supplementary Methods for more details.

Protein lysates and Western blotting

Transfected MC4 cell cultures were treated with 1× lysis buffer (Cell Signaling) to make whole-cell lysates, which were examined by Western blotting with primary antibodies as indicated. The membranes were then incubated with secondary chemiluminescent antibodies and imaged using a ProteinSimple FluorChem M imaging system. Quantitation of protein band densities was performed using the alpha view analysis software package.

Real-time quantitative PCR RNA expression analyses

MC4 RNA was isolated using TRIzol reagent and converted to cDNA using First-Strand cDNA Synthesis System (Life Technologies, 11904-018). qPCR was carried out using 2× Maxima SYBR Green/ROX *q*PCR Master Mix (K0223, Thermo Fisher) in Fast 96-Well Reaction Plates (Applied Biosystems) using a StepOnePlus (Applied Biosystems). Relative mRNA levels were calculated using the $\Delta\Delta C_t$ method using *18SrRNA* for normalization. The qPCR primers are listed in Supplementary Table S1.

ChIP assay

Chromatin from MC4 cells, MM-BMSC, and HD-BMSC was analyzed using a modification of the ChIP Millipore/Upstate protocol (MCPROTO407) as described (29) using Magna ChIP Protein A+G Beads (16-663, Millipore). In brief, a total of 2×10^7 cells were fixed in 1% formaldehyde (F79-500, Fisher) for 10 minutes at room temperature. Samples were sonicated (to generate DNA fragments of 250 base pairs average length) on ice using a Fisher Scientific Sonic Dismembrator (Model 100) and centrifuged at 12,000 rpm for 10 minutes. Chromatin from 4×10^6 cells was diluted 7-fold in ChIP Dilution Buffer (0.01% SDS, 1.1% Triton X-100, 1.2 mmol/L EDTA, 16.7 mmol/L Tris-HCl, pH8.1, 167 mmol/L NaCl) and incubated at 4°C overnight with respective antibodies. Aliquots for input and nonspecific IgG control samples were included with each experiment. IgG ChIP was run on untreated MC4 samples. ChIP-qPCR primers are listed in Supplementary Table S2. Fold enrichment was calculated on the basis of C_t as $2^{(\Delta Ct)}$, where $\Delta C_t = (C_{t\_Input} - C_{t\_IP})$. The IgG ΔC_t was subtracted from the specific Ab ΔC_t to generate $\Delta\Delta C_t = (\Delta C_{t\_specific\ Ab} - \Delta C_{t\_IgG})$.

Statistical analysis

All experiments were repeated at least 2 independent times. Most data are presented as biologic triplicates and results reported as means ± SD unless otherwise stated. Statistical significance was evaluated by either the Student *t* test or one-way ANOVA with Tukey multiple comparison posttest using GraphPad Prism 6 as indicated. Degree of significance is represented using ρ values: *, $\rho \leq 0.05$; **, $\rho \leq 0.01$; ***, $\rho \leq 0.001$; ****, $\rho \leq 0.0001$. (Different symbols may be used to reflect multiple 2-way comparisons.)

Results

Multiple myeloma induces sustained transcriptional and epigenetic suppression of the m*Runx2* promoter in murine pre-osteoblast cells

We (Supplementary Fig. S1) and others (30) demonstrated that multiple myeloma cells and TNFα cause a very rapid decrease of *Runx2* mRNA mediated by decreasing *Runx2* mRNA half-life. However, as maintenance and propagation of gene silencing are often controlled at the chromatin level, we hypothesized that the long-term suppression of osteoblast differentiation in the multiple myeloma microenvironment results from epigenetic repression of *Runx2* transcription in BMSCs. Therefore, we analyzed the effect of 5TGM1-MM cell exposure on RNA polymerase II (Pol II) occupancy and the histone H3 methylation and acetylation profiles along the murine (m)*Runx2* locus during MC3T3-E1 subclone-4 (MC4) cell proliferation and osteoblast differentiation (Fig. 1A) using ChIP-qPCR (Fig. 1B) amplicons as indicated. We found that MC4 exposure to 5TGM1 inhibited the osteoblast-induced recruitment of Pol II to the m*Runx2-P1* promoter (Fig. 1C, amplicons 3 and 4), as well as decreased elongating Pol II (marked by Ser2 phosphorylation of the C-terminal domain; Ser2P CTD) downstream of the m*Runx2-P1* promoter (Fig. 1D), thus demonstrating that multiple myeloma exposure downregulates m*Runx2* transcription in MC4 cells. Paused Pol II was not evident at the m*Runx2-P2* promoter (Fig. 1C, amplicons 8ABC), but transiting Pol II was elevated by osteoblast differentiation and decreased by multiple myeloma exposure (Fig. 1D). Further evidence of prior multiple myeloma exposure leading to inhibition of m*Runx2* transcription during osteoblast induction is revealed by decreased enrichment of trimethylated H3K36 (H3K36me3) toward the 3′ end of the m*Runx2* gene (Fig. 1E), which marks the Pol II elongation footprint (31). However, multiple myeloma exposure did not affect presence of Pol II, Ser2P CTD, and H3K36me3 at m*Runx2* in proliferating MC4 (Fig. 1C–E). The permissive chromatin marks, acetylation at H3K9 (H3K9ac; Fig. 1F) and methylation at H3K4 (H3K4me3; Fig. 1G), were abundant at both m*Runx2* promoters prior to osteoblast stimulus, reflecting the poised and basal/constitutive transcription levels in MC4 cells. These marks increased following differentiation (more so at *P1* than at *P2*), consistent with increased m*Runx2* activation. Multiple myeloma exposure significantly reduced the H3K9ac and H3K4me3 levels at m*Runx2-P1* in proliferating MC4 (d0) and they were

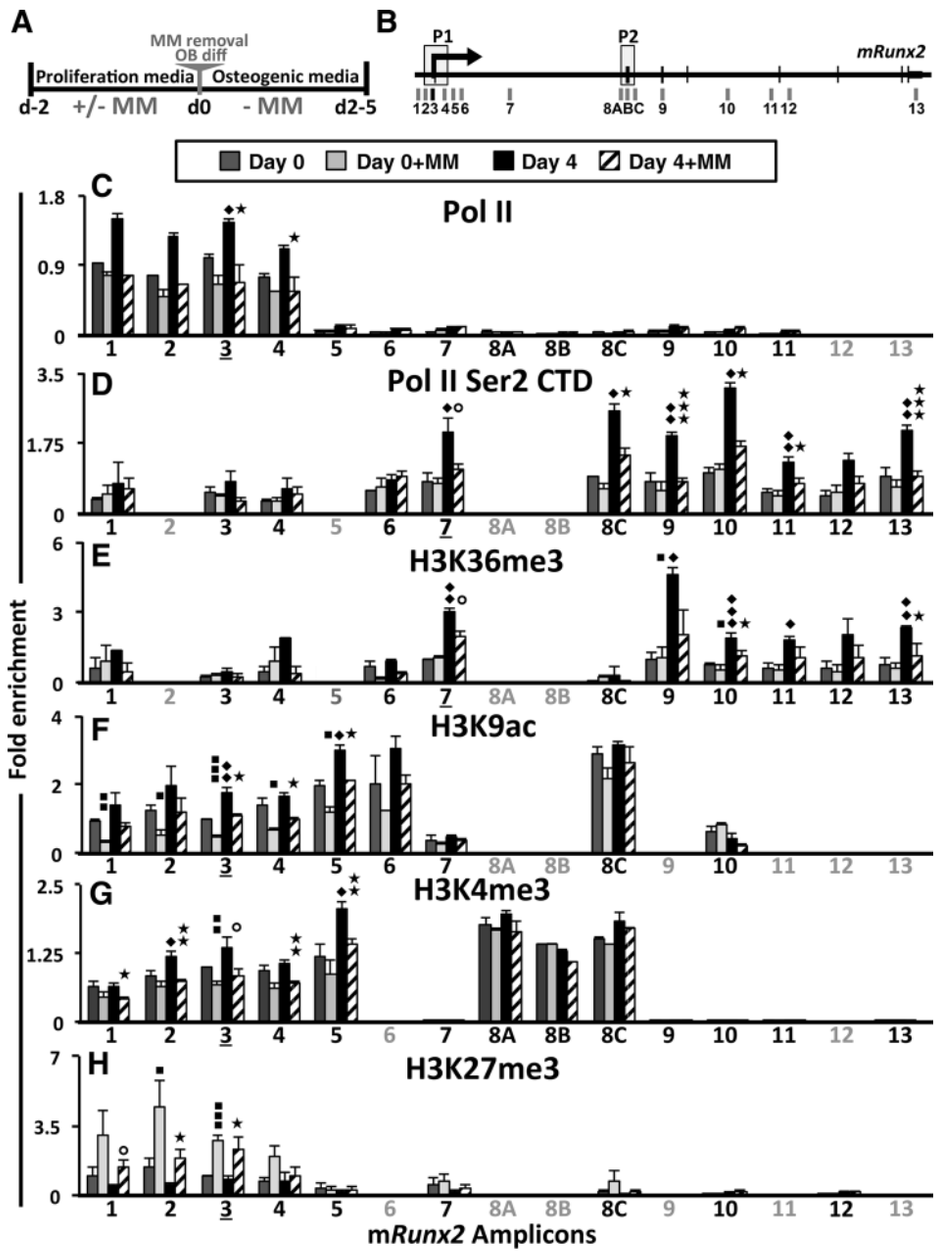

Figure 1.
Transcriptional and epigenetic changes at *mRunx2* in multiple myeloma–exposed MC4. **A,** Experimental design schematic of 5TGM1-MM-MC4 co-cultures and induction of osteoblast differentiation. After 48-hour co-culture in proliferation media, the multiple myeloma cells were removed, and the MC4 were either harvested immediately (d0 ± MM) or first placed in osteoblast differentiation media for 4 days (d4 ± MM). **B,** Schematic of *mRunx2 q*PCR amplicons with promoters P1 and P2 indicated (see Supplementary Table S2 for positional numbering and the primer sequences). Amplicon-3 encompasses the Gfi1-binding site. **C–H,** ChIP-qPCR analyses of RNA Pol II occupancy and several H3 modifications along *mRunx2* in MC4 cells treated as described in **A** using qPCR amplicons denoted in **B** (amplicons not done for a particular pull-down are in gray). Enrichment values are plotted relative to amplicons 3 or 7 as indicated by underlining, depending upon whether the focus was on the promoter (**C**, **F–H**) or the body of the gene (**D**, **E**): (**C**) total RNA Pol II; (**D**) phosphorylated Pol II CTD Ser 2P; (**E**) elongation mark H3K36me3; (**F**) activation mark H3K9ac; (**G**) activation mark H3K4me3; and (**H**) repressive mark H3K27me3. Error bars represent SEM of 3 to 4 biological replicates (2 replicates for H3K9ac d4 ± multiple myeloma). Statistically significant comparisons of: ♢, d4 − MM to d0 − MM; ■, d0 + MM to d0 − MM; ★, d4 + MM to d4 − MM. ○, values of $P < 0.08$.

refractory to elevation by osteoblast differentiation induction (d4). In contrast, multiple myeloma cells upregulated m*Il6* mRNA in proliferating MC4, with increased Pol II occupancy and H3K9ac, H3K4me3, and H3K36me3 levels at the m*Il6* gene (Supplementary Fig. S2). There is more of the repressive H3K27 trimethylation (H3K27me3; ref. 32) mark on the m*Runx2-P1* promoter than m*Runx2-P2* in proliferating cells (Fig. 1H), reflecting the bivalent nature of the poised *P1* promoter. Furthermore, multiple myeloma increased H3K27me3 only at the m*Runx2-P1* promoter in MC4 (Fig. 1H), which remained elevated 4 days after multiple myeloma cell removal. These data indicate that multiple myeloma exposure reduced the transcriptionally permissive bivalent chromatin architecture of the m*Runx2-P1* promoter in MC4 cells, marked by high H3K9ac and H3K4me3 levels along with H3K27me3, and induced a more repressive H3K27me3-prevalent signature.

Myeloma induces recruitment of GFI1 to the m*Runx2* promoter in pre-osteoblast

As we had shown an inverse correlation with GFI1 levels and *Runx2* expression (6), we postulated that GFI1 is directly responsible for the multiple myeloma–induced epigenetic changes by binding at the *Runx2* gene and recruiting various corepressors to establish epigenetic silencing. Therefore, we first needed to establish whether GFI1 binds the *Runx2* gene. Using Gfi1-WT cotransfections with a set of 5′ and 3′ deletions, as well as internal deletions, of m*Runx2*-pGL4.10[luc2] reporters, we localized the GFI1 responsivity to the −37/−7 region

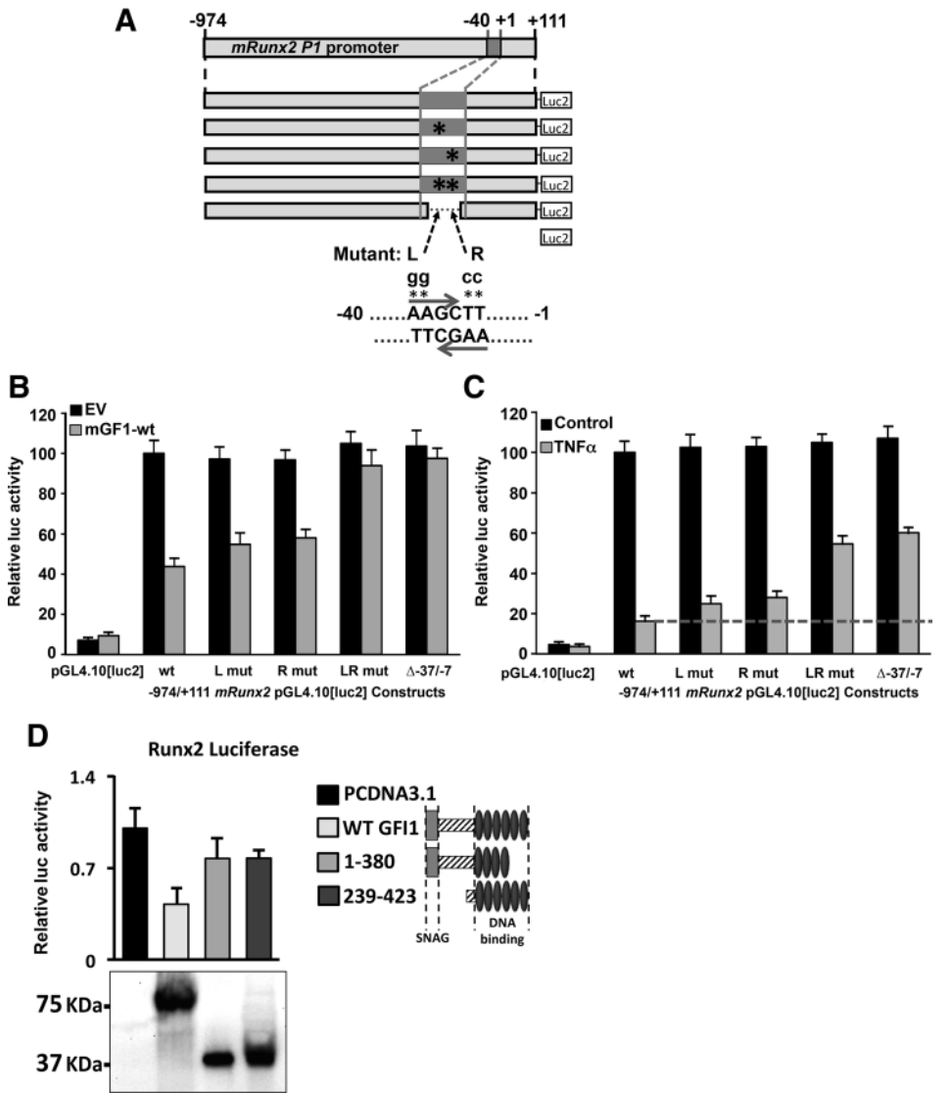

Figure 2.
Mutation of the GFI1 cores at −21/−16 *mRunx2* relieves ectopic GFI1 and TNFα repression of the *Runx2* promoter. Reporters −974/+111 *mRunx2* promoter-pGL4.10[luc2] WT or containing mutations L, R, or LR or the internal deletion Δ−37/−7 (depicted in **A**) were transfected into MC4 cells either (**B**) with pcDNA3.1 (EV) and pcDNA3.1-mGFI1-WT plasmids or (**C**) that were treated with nothing (Control) or TNFα (0.5 ng/mL) 6 hours after transfection. **B** and **C,** Reported luciferase activities in harvested (48 hours) cell lysates were evaluated with respect to WT reporter either (**B**) cotransfected with EV or (**C**) the untreated control. **D,** Myc-mGFI1-WT, deletion constructs which encode mGfi1 aa 1–380 or 239–423, and EV were cotransfected into MC4 cells with *mRunx2*-Luc-WT reporter depicted in **A**, and harvested lysates were analyzed for luciferase activities as compared with cells transfected with EV and myc-GFI1 expression by Western blotting (shown below graph). Each experiment above was repeated at least 3 independent times.

(Supplementary Fig. S3A and S3B). There is no consensus GFI1-binding site (15, 19) in the −108/−1 m*Runx2* promoter, but the region contains 6 GFI1-binding site cores (AA(T/G)C). Therefore, we used a combination of biotin-oligo (B-oligo) streptavidin agarose bead pull-down assays (Supplementary Fig. S3C–S3G) and electrophoretic mobility shift assay (Supplementary Fig. S3H and S3I) to establish that GFI1 binds at an overlapped palindromic pair of GFI1 cores at −21/−18 (L) and −19/−16 (R). Mutation of either core decreased GFI1 binding, but mutation of both (LR) ablated binding (Supplementary Fig. S3G and S3H). GFI1 cotransfected into MC4 with −974/+111 m*Runx2*-pGL4.10[luc2] reporters containing site-specific mutations (L, R, and LR) of the −21/−16 double core GFI1-binding site (Fig. 2A) showed that the 2 single-site m*Runx2* mutants (L, R) were partially resistant to GFI1, and the double LR mutant and the Δ−37/−7 m*Runx2* deletion were entirely resistant (Fig. 2B). Similar results with this set of m*Runx2* reporters were obtained using TNFα treatment to repress m*Runx2* (Fig. 2C), although the rescue from TNFα repression is only about 60% with LR or Δ−37/−7. This may indicate that a weaker GFI1-binding site at −67/−64 may also play a role in TNFα repression of *Runx2* or that another factor is involved. Western blot analysis of the expression of transfected GFI1 protein deletions in HEK293 cells established that the mutant myc-mGFI1 proteins were all expressed as well or better than mGFI1-WT (Input) and −40/−1 B-oligo pull-downs using these extracts demonstrated that only mGFI1-WT and mGFI1;239-423 bound DNA (Supplementary Fig. S4A). Cotransfection of mGFI1-WT, mGFI1;239-423 (lacking recruitment domains for many corepressors) and mGFI1;1-380 (lacking the C-terminal 43aa and does not bind DNA) expression plasmids with the −974/+111 m*Runx2*-pGL4.10[luc2] reporter revealed that neither mutant mGFI1 could repress reporter expression, although they were expressed at similar levels as mGFI1-WT (Fig. 2D).

Consistent with the reporter experiments, we observed that ectopic mGFI1 dose dependently decreased endogenous m*Runx2* mRNA in proliferating undifferentiated MC4 cells (Fig. 3A), indicating that increased GFI1 was sufficient for endogenous m*Runx2* repression. The increased GFI1 did not

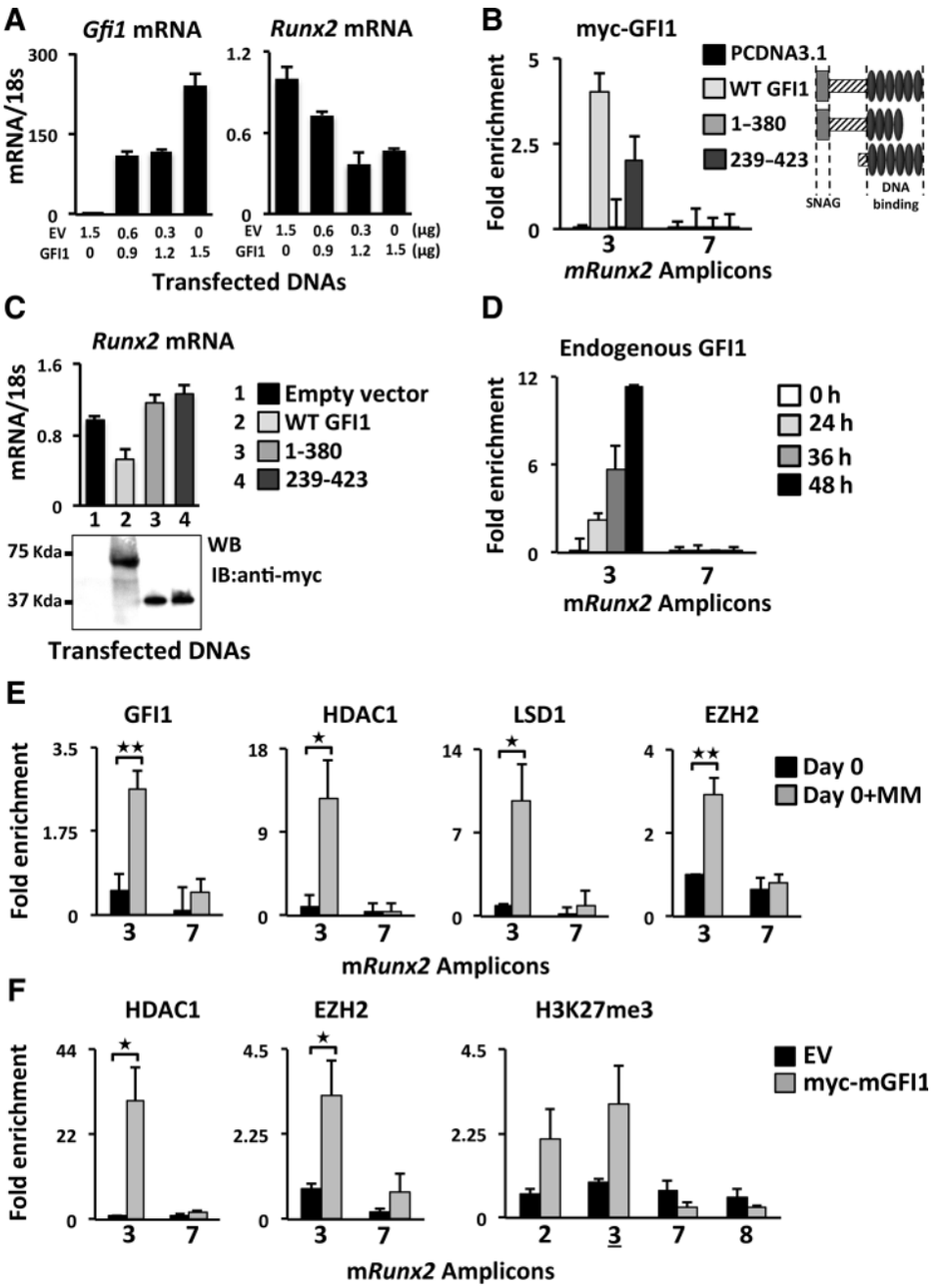

Figure 3.

Analysis of recruitment to m*Runx2* of histone modifier enzymes in multiple myeloma–exposed or GFI1-transfected MC4. **A,** Varying amounts of mGFI1-WT and EV plasmids transfected as indicated into MC4 cells and m*Gfi1* and endogenous m*Runx2* mRNA levels were evaluated by qPCR. **B** and **C,** Myc-mGFI1-WT, myc-mGFI1 deletion constructs encoding aa 1–380 or 239–423, or EV were transfected into MC4. Transfected cells were analyzed for (**B**) myc-mGFI1 binding at the *Runx2* promoter amplicon-3 by ChIP-qPCR using anti-myc Ab and (**C**) the effect on endogenous *Runx2* mRNA levels by qPCR with expression of the transfected myc-mGFI1s by Western blot analysis displayed underneath. **D,** ChIP-qPCR analysis of endogenous GFI1 recruitment to the *Runx2* promoter amplicon-3 (Fig. 1B) in MC4 cells co-cultured with 5TGM1-MM cells for the indicated times. For all, biologic triplicates within 2 separately run experiments were averaged together and the SEM calculated. **E,** ChIP-qPCR analyses of MC4 cells after multiple myeloma exposure per scheme in Fig. 1A (d0 ± MM) for GFI1 binding and HDAC1, LSD1, and EZH2 occupancy within the *mRunx2* amplicon-3. **F,** ChIP-qPCR analyses of ectopic GFI1 recruitment of HDAC1 and EZH2 and consequent enhancement of H3K27me3 at the *Runx2* promoter in MC4. Error bars represent SEM for 3 biologic replicates except H3K27me3 in **F** had only 2. **B**, **D–F**, Amplicon-7 was used as a negative control for GFI1 binding.

alter expression of *Sp1*, *Il6*, or the RUNX2 targets *Osx (Sp7)*, *Ocn*, and *Bsp* (Supplementary Fig. S4B); the latter because these genes were not yet stimulated. We analyzed the capacity of ectopic mGFI1-WT and mGFI1 deletions (1–380 and 239–423) to bind (Fig. 3B) and regulate endogenous m*Runx2* expression (Fig. 3C). ChIP-qPCR analysis demonstrated ectopic mGFI1-WT and mGFI1;239-423 occupancy on the endogenous m*Runx2* promoter in MC4 cells using amplicon-3 (centered on −36) that included the −21/−16 GFI1 sites whereas mGFI1;1-380 did not bind (Fig. 3B). Furthermore, mGFI1-WT repressed endogenous mRunx2 expression; while neither mGFI1;1-380 nor mGFI1;239-423 was able to repress m*Runx2* expression (Fig. 3C). A ChIP-qPCR scan for ectopic GFI1-WT binding along the *Runx2* gene showed that it did not bind near the *Runx2-P2* promoter (Supplementary Fig. S4C). Kinetic ChIP-qPCR analyses of multiple myeloma–exposed MC4 cells revealed that endogenous GFI1 recruitment to m*Runx2-P1* is not detectable until 36 hours of multiple myeloma treatment with increased occupancy at 48 hours (Fig. 3D).

GFI1 recruits chromatin corepressors to induce epigenetic suppression of the *Runx2* promoter in myeloma-exposed pre-osteoblast

The pleiotropic effects of GFI1-targeted epigenetic gene repression are associated with its recruitment of various histone

corepressors (20, 21, 33). Because we demonstrated that multiple myeloma cells induce recruitment of endogenous GFI1 to the *Runx2* gene (Fig. 3D and E) with concomitant epigenetic repression of the *Runx2* locus (Fig. 1C–H), we screened for multiple myeloma–induced occupancy of chromatin modifiers near the GFI1-binding site in m*Runx2* in pre-osteoblasts. Multiple myeloma treatment induced HDAC1 and LSD1 (Fig. 3E) binding to the m*Runx2* promoter in MC4 cells, which is consistent with the observed decrease in transcription activation marks H3K9ac and H3K4me3 (Fig. 1). Because we detected a significant multiple myeloma–induced increase in H3K27me3 levels at m*Runx2* (Fig. 1H), we used ChIP to confirm multiple myeloma–induced occupancy of EZH2, the methyltransferase component of the polycomb repressive complex 2 (PRC2) responsible for generating H3K27me3 (34), near the m*Runx2* GFI1-binding site (Fig. 3E).

Ectopically expressed Myc-mGFI1-WT in MC4 cells resulted in recruitment of the histone modifiers HDAC1 and EZH2 to the *mRunx2* amplicon-3 (Fig. 3F), thus demonstrating that GFI1 is capable of recruiting these corepressors to m*Runx2* in the absence of multiple myeloma signals. Furthermore, the increased recruitment of endogenous EZH2 resulted in enhanced deposition of the repressive H3K27me3 mark (Fig. 3F).

GFI1 is required for multiple myeloma–induced recruitment of repressive chromatin modifiers to the *Runx2* gene in pre-osteoblast

The direct involvement of multiple myeloma–induced GFI1 recruitment of epigenetic corepressors was further delineated using a stable *Gfi1*-knockdown MC4 cell line (shGfi1-MC4; Fig. 4A), with approximately 50% reduction in GFI1 protein levels (Supplementary Fig. S4D). 5TGM1-MM co-culture with control shSCR-MC4 resulted in the expected reduction of m*Runx2* mRNA expression (Fig. 4B). Multiple myeloma co-culture with shGfi1-MC4 still resulted in a rapid decrease in m*Runx2* mRNA (Fig. 4B d0), likely due to mRNA destabilization. However, decreased GFI1 prevented the sustained m*Runx2* repression observed following induction of osteoblast differentiation (Fig. 4B d4). Furthermore, RUNX2 target genes m*Ocn* and m*Bsp* also exhibited significant resistance to multiple myeloma inhibition in shGfi1-MC4 compared with SCR-MC4 (Fig. 4C and D). Alkaline phosphatase (m*Alpl*) expression trended up, but the change was not significant (Fig. 4E). Consistent with the multiple myeloma–resistant m*Runx2* mRNA expression in shGfi1-MC4, lack of multiple myeloma–induced GFI1 binding to the m*Runx2* promoter (Fig. 4F) results in deficient recruitment of corepressors HDAC1 (Fig. 4G) and EZH2 (Fig. 4H). Furthermore, lack of GFI1-mediated HDAC1 and EZH2 recruitment rescued levels of H3K9ac at m*Runx2* after multiple myeloma co-culture (Fig. 4I). Concomitantly, we observed significantly reduced enrichment of the repressive mark H3K27me3 (Fig. 4J), further arguing for the importance of GFI1-directed EZH2 recruitment to the m*Runx2* promoter in pre-osteoblast during multiple myeloma co-culture conditions. Thus lack of GFI1 recruitment directly correlates with the inability of the multiple myeloma cells to induce epigenetic suppression of the m*Runx2* promoter. These results reveal that destabilization of m*Runx2* mRNA is not sufficient to prevent osteoblast differentiation in the absence of GFI1-mediated epigenetic alteration of the m*Runx2* gene.

Multiple myeloma suppression of m*Runx2* and osteoblast differentiation of MC4 cells is reversed by HDAC1 or EZH2 inhibition.

We used small-molecule inhibitors of HDAC1 (MC1294) and EZH2 (GSK126) enzymatic activities to investigate whether the multiple myeloma–induced GFI1-mediated epigenetic repression of m*Runx2* is reversible. Following 5TGM1-MC4 co-cultures in proliferation media, we removed the multiple myeloma cells and subjected the MC4 cells to osteoblast differentiation in the presence of vehicle, MC1294, or GSK126 (Fig. 5). Western blot analyses demonstrated that the HDAC inhibitor MC1294 increased global H3K9Ac levels in MC4 cells after 2 days regardless of whether or not the cells had been pre-exposed to multiple myeloma cells, while not affecting the H3, HDAC1, EZH2, or H3K27me3 levels (Fig. 5A). Similarly, the EZH2 inhibitor GSK126 decreased global H3K27me3 levels in MC4 cells after 2 days without affecting H3, EZH2, HDAC1, and H3K9ac levels (Fig. 5B). MC4 treatment with MC1294 or GSK126 did not alter standard osteoblast differentiation–stimulated m*Runx2* mRNA expression at d4 (Fig. 5C). However, inhibition of HDAC1 or EZH2 activity significantly rescued m*Runx2* mRNA from the multiple myeloma–mediated sustained repression at d4 (Fig. 5C). HDAC1 and EZH2 inhibition similarly rescued mRNA expression of several downstream RUNX2 targets critical for osteoblast differentiation, including m*Ocn*, m*Bsp*, and m*Alpl* (Fig. 5D–F). Mineralization assays confirmed that EZH2 inhibition reversed the osteoblast differentiation block established by human MM1.S Transwell co-culture with MC14 cells (Fig. 5G). Our results argue that GFI1 recruitment of the epigenetic histone modifiers HDAC1 and EZH2 and their actions at the *mRunx2* histones facilitate the suppressive multiple myeloma effects on *mRunx2* in pre-osteoblast MC4 cells and that this effect is reversible after short-term (48–72 hours) multiple myeloma exposure.

Multiple myeloma induces sustained transcriptional and epigenetic suppression of the h*Runx2* promoter in human multiple myeloma patient BMSC that is reversed by HDAC1 or EZH2 inhibition

To demonstrate involvement of multiple myeloma–induced h*Runx2* epigenetic suppression in preventing osteoblast differentiation in patients, we used ChIP-qPCR to analyze the activation mark H3K9ac at the h*Runx2* promoter in BMSCs from patients with multiple myeloma (MM-BMSC) and healthy donors (HD-BMSC). Chromatin isolated from MM-BMSC ($n = 12$) revealed significant reduction of H3K9ac at the h*Runx2* promoter as compared with HD-BMSC samples ($n = 6$; Fig. 6A). Analysis of additional samples demonstrated that the repressive mark H3K27me3 at the h*Runx2* promoter was higher on average for MM-BMSC ($n = 12$) than HD-BMSC ($n = 6$; Fig. 6B), although the difference did not reach statistical significance. Therefore, we treated MM-BMSC from 2 patients with vehicle, MC1294, or GSK126 for 7, 14, and 21 days in osteogenic culture conditions and assayed mineralization/calcium deposition (Fig. 6C and D). Both MC1294 and GSK126 permitted significantly more osteoblast differentiation as compared with vehicle for each MM-BMSC sample. MM-BMSCs from 3 additional patients assayed only at 21 days gave similar results (Supplementary Fig. S5A–S5D). In contrast, EZH2 inhibition did not change osteoblast differentiation of HD-BMSC (Supplementary Fig. S5E). These data, together with our results

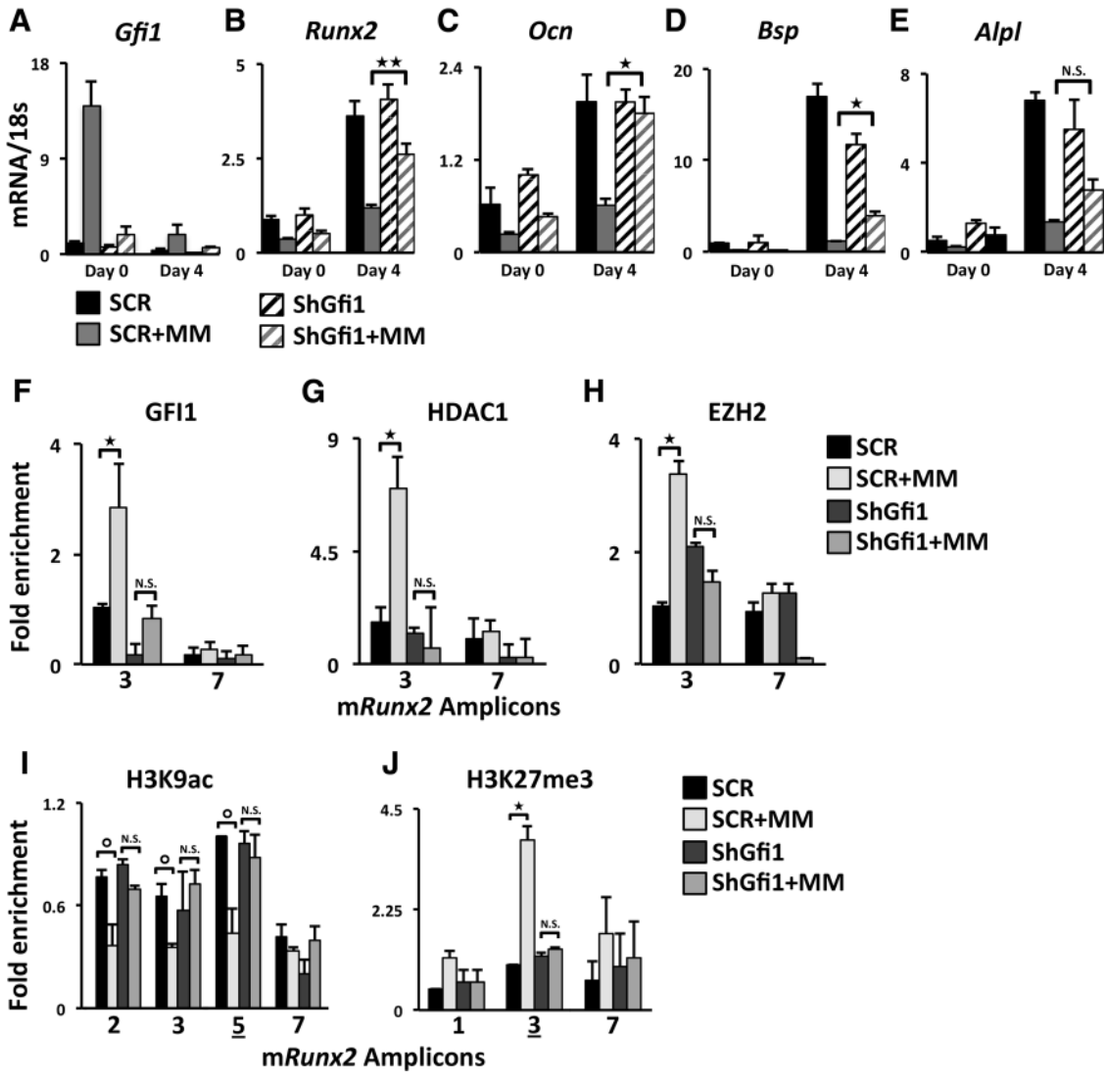

Figure 4.

m*Gfi1* knockdown in MC4 cells prevents multiple myeloma–induced repression of m*Runx2* and osteoblast differentiation markers, the recruitment of HDAC1 and EZH2, and repressed chromatin architecture acquisition. q*PCR* analysis of mRNAs from SCR- and shGfi1-MC4 cells treated as described in Fig. 1A for (**A**) *Gfi1*, (**B**) *Runx2*, (**C**) *Ocn*, (**D**) *Bsp*, and (**E**) *Alpl* mRNA expression. ChIP-qPCR analyses of multiple myeloma–induced recruitment to the *Runx2* promoter of (**F**) GFI1, (**G**) HDAC1, and (**H**) EZH2 and enrichment profiles for (**I**) H3K9ac and (**J**) H3K27me3 in SCR and shGfi1-MC4 at d0 ± MM. IgG ChIP was run on SCR-MC4 cells. Error bars represent SEM for (**A–E**) 3–4 or (**F–J**) 2 biologic replicates. o, values of $P < 0.08$. Amplicons as indicated in Fig. 1B.

from MC4 cells (Fig. 5), demonstrate that multiple myeloma–induced GFI1 recruitment of EZH2 mediates H3K27me3 epigenetic repression of *Runx2*, which contributes to the long-term suppression of hBMSC differentiation into functioning osteoblast, and, importantly, that it is reversible even after long-term multiple myeloma exposure *in vivo*.

Discussion

Our studies demonstrate that the key mechanism by which multiple myeloma cells establish persistent suppression of osteoblast differentiation in MMBD (5) is via induction of direct GFI1 binding to the *Runx2-P1* promoter in pre-osteoblast cells resulting in *Runx2* repression. While multiple myeloma cells enhance *Runx2* mRNA degradation in proliferating pre-osteoblast, this effect is not sufficient to establish osteoblast suppression. Multiple myeloma cells induce GFI1 binding to a novel GFI1 response element within the *Runx2-P1* promoter. GFI1 then acts as a platform molecule for formation of a repressive complex containing histone modifier enzymes HDAC1, LSD1, and EZH2, which decrease H3K9ac and H3K4me3 and increase H3K27me3 modifications, respectively, to establish a repressive chromatin architecture at *Runx2* that is refractory to osteoblast inducer activation (Fig. 7). Importantly, we have shown that this refractory state requires active maintenance and is reversible by inhibition of HDAC1 or EZH2 activity.

We identified a functional GFI1 response element with 2 overlapped palindromic cores at −21/−16, that each

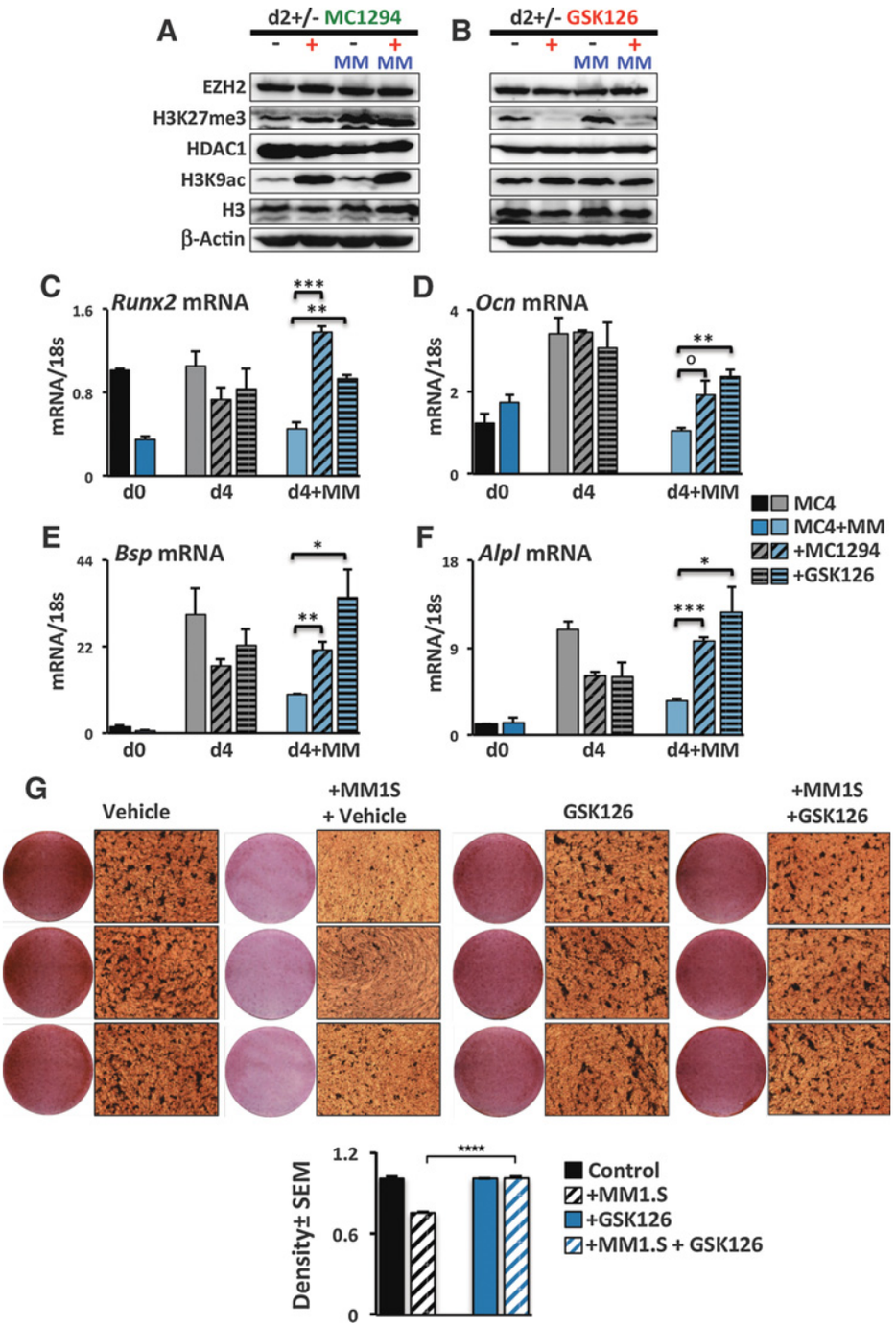

Figure 5.
Inhibition of histone modifiers HDAC1 and EZH2 rescues osteoblast differentiation of multiple myeloma–exposed MC4 cultures. **A–F,** MC4 cells were exposed to 5TGM1-MM cells as diagrammed in Fig. 1A in the absence of inhibitors. After multiple myeloma removal at d0, the MC4 cells were cultured in osteoblast differentiation media for 2 to 4 days with either vehicle, MC1294 (10 μmol/L), or GSK126 (5 μmol/L) added as indicated. **A** and **B,** Effects of the inhibitors (**A**) MC1294 (HDACi) and (**B**) GSK126 (EZH2i) on global levels of H3K9ac, H3K27me3, H3, HDAC1, EZH2 levels in MC4 cells on day 2 were assessed by Western blotting using antibodies as indicated. **C–F,** Effects of the inhibitors MC1294 and GSK126 on (**C**) *Runx2*, (**D**) *Ocn*, (**E**) *Bsp*, and (**F**) *Alpl* mRNA expression during differentiation of control and 5TGM1-MM–exposed MC4 at day 0 (no inhibitor) or after 4 days of differentiation (d0 ± MM, d4 ± MM). Error bars represent SEM for 3 biologic replicates. **G,** Human MM1.S multiple myeloma cells in Transwells (or empty control Transwells) were co-cultured with MC14 cells for 72 hours. Following Transwell removal, the MC14 cells were cultured in osteogenic media ± GSK126 (2.5 μmol/L), and mineralization was assessed using alizarin red staining at d21; the GSK126 was absent days 14 to 21. Shown is density quantitation for the average of 6 wells with SEM and significance indicated.

contributes to the strength of GFI1 binding. It is possible that the presence of both sides of the palindromic recognition sites generates some cooperative binding, although this is unlikely to be through Zn fingers 3–5 of 2 GFI1 molecules interacting with the DNA at the same time due to steric hindrance (19, 35, 36). GFI1 has not been reported to dimerize, although other C2H2 Zn finger transcription factors, such as Ikaros, TRPS1, and Drosophila Hunchback can homodimerize via the alpha helices of 2 Zn fingers that are not involved in protein–DNA interactions (37). It remains to be established whether these palindromic sites can induce a pair of GFI1 molecules to bind at the same time, perhaps by each only contributing a subset of Zn fingers 3–5.

Gene expression is closely associated with histone exchange and histone posttranslational modifications, which regulate the states of chromatin compaction and assembly of transcription machinery at gene promoters (38). In proliferating pre-osteoblast, we found that the *Runx2-P1*

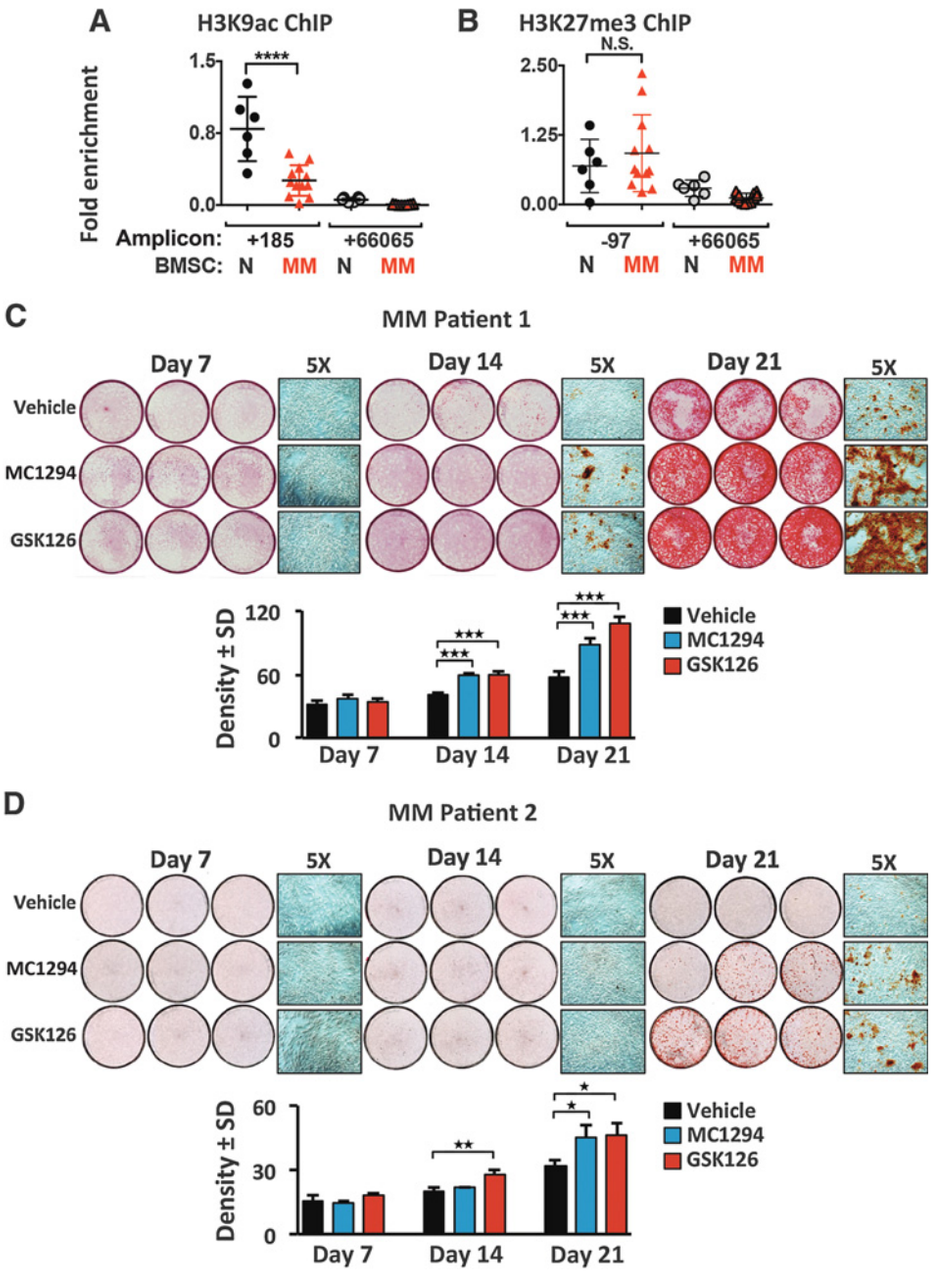

Figure 6.
MM-BMSC samples exhibited decreased H3K9Ac at the h*RUNX2* promoter compared with HD-BMSC and inhibition of either HDAC1 or EZH2 rescues MM-BMSC osteoblast differentiation. **A,** Anti-H3K9Ac (and IgG) ChIP-qPCR analysis of HD-BMSC (N; $n = 6$) and MM-BMSC (MM; $n = 12$, patient characteristics in Supplementary Table S3) using amplicons +185 and +66,065 relative to the h*RUNX2* P1 TSS. One anti-H3K9Ac ChIP amplicon +185 N sample result was used as the reference sample for all other data and $\Delta\Delta C_t$ shown. **B,** Anti-H3K27me3 (and IgG) ChIP-qPCR analysis of HD-BMSC ($n = 6$), which included 2 donors used in **A**, and a unique set of MM-BMSC ($n = 12$, patient characteristics in Supplementary Table S4), using amplicons −97 and +66,065 as described in **A**. There were no significant differences in the IgG pull-down results across all samples and between the amplicons. The significance of differences between N and MM samples for each amplicon were determined by one-way ANOVA with Tukey multiple comparison posttest using GraphPad Prism 6. **C** and **D,** MM-BMSC from 2 different patients (Supplementary Table S5) were cultured 7, 14, or 21 days in osteogenic media supplemented with vehicle, MC1294 (10 μmol/L), or GSK126 (2.5 μmol/L); the inhibitors were absent on days 14 to 21. Mineralization was assessed using alizarin red staining. Three independent wells from each treatment group are shown as well as a representative 5× magnification. Below each set is the density quantitation for the average of 6 wells per condition with SEM and significance indicated.

promoter has a poised bivalent chromatin architecture with moderate levels of active histone marks H3K9ac and H3K4me3, as well as the repressive mark H3K27me3, is preloaded with Pol II, and undergoes a low level of basal transcription detectable by qPCR. Many developmental genes have a similar poised promoter architecture that can swiftly respond to external stimuli but lacks the transcription elongation properties associated with active gene expression (39). Similar to a previous report (40), stimulation of osteoblast differentiation induced changes in the *Runx2* epigenetic profile (increased H3K36me3, H3K9ac, and H3K4me3 and decreased H3K27me3) that were consistent with the expected activation of the *Runx2* gene.

We found that multiple myeloma cells induced significant chromatin alterations on the *Runx2* gene in pre-osteoblast cells in proliferation media that included a profound decrease in the activation mark H3K9ac together with increased levels of the repressive mark H3K27me3. ChIP-qPCR of human BMSC samples from patients with multiple myeloma and healthy donors also revealed significantly decreased H3K9ac and a trend toward higher H3K27me3 in MM-BMSC than in HD-BMSC. H3K27me3 has been reported to be elevated in primary undifferentiated BMSC, with removal by the demethylase Jumonji domain–containing protein 3 (JMJD3) required to allow *Runx2* activation during osteoblast induction (41). Thus, the difference in H3K27me3 levels between MM-BMSC and HD-BMSC after

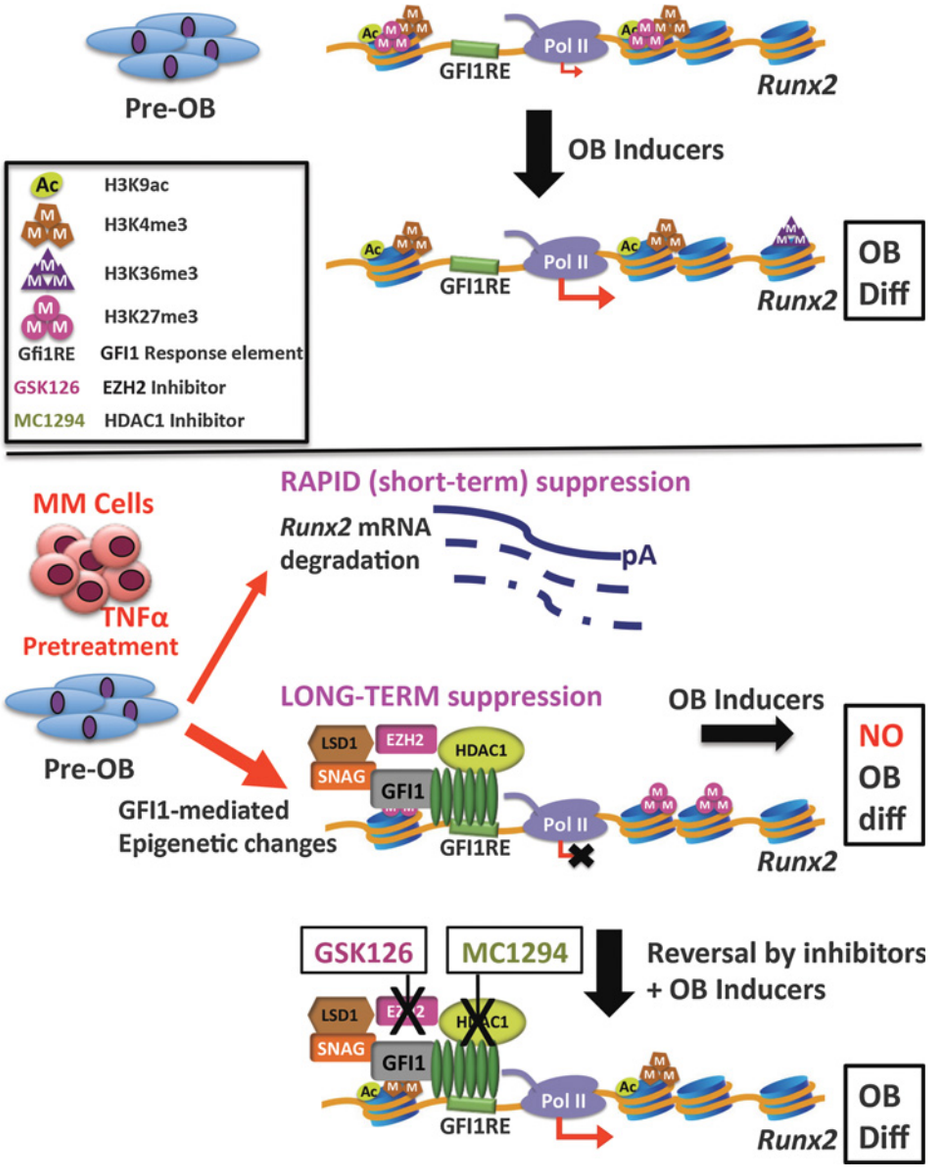

Figure 7.
Schematic of the mechanism of GFI1-induced epigenetic repression of the *Runx2* locus in multiple myeloma–exposed pre-osteoblast. In proliferating pre-osteoblast cells, *Runx2-P1* is in a poised bivalent configuration with paused Pol II and prominent levels of activation-ready promoter chromatin marks H3K4me3 and H3K9ac, as well as H3K27me3, with low levels of basal transcription. Osteoblast differentiation induction stimulates increased accumulation of these active chromatin marks, as well as release of Pol II into the *Runx2* structural region as marked by increased Pol II Ser2P-CTD and accumulation of the H3K36me3 mark. Multiple myeloma exposure acts in a dual mode to repress *Runx2* expression. The rapid TNFα-induced decrease in *Runx2* mRNA is mediated by increased mRNA degradation. However, this is insufficient to block induction of osteoblast differentiation. The sustained suppression of osteoblast differentiation requires modifications of the *Runx2* chromatin architecture. GFI1 binds to *Runx2* and facilitates recruitment of histone corepressors HDAC1, LSD1, and EZH2, which results in decreased active H3K9ac and H3K4me3 and increased repressive H3K27me3 chromatin marks, causing an epigenetic block refractory to transcriptional activation in response to osteoblast differentiation signals. Inhibition of either HDAC1 or EZH2 can reverse the inhibition and allow osteoblast differentiation.

osteoblast differentiation induction would likely be larger. In summary, the effect of these multiple myeloma–induced chromatin changes in proliferating pre-osteoblast is to make the *Runx2* gene refractory to activation by osteoblast differentiation stimulation, even in the absence of multiple myeloma cells, by blocking the normal epigenetic changes induced during osteoblast differentiation. Thus, leaving the *Runx2* chromatin in a state similar to the undifferentiated, proliferating pre-osteoblast despite of exposure to activation signals.

ChIP-qPCR analysis of MM-MC4 co-culture time courses revealed that GFI1 recruitment to the *Runx2-P1* promoter is not rapid, taking at least 36 hours to become detectable. This result supports our previous report that GFI1 translocates from the cytoplasm to the nucleus following 5TGM1-MM co-culture or TNFα treatment of more than 24 hours (6). Multiple myeloma–induced GFI1 recruitment to the *Runx2* promoter coincided with an increased presence of LSD1, HDAC1, and EZH2, the enzymes responsible for the histone modifications that established an epigenetic block to osteoblastogenesis. Ectopic expression of GFI1 in MC4 cells in the absence of multiple myeloma exposure was sufficient to recruit HDAC1 and EZH2, alter the chromatin architecture, and repress the *Runx2* gene. GFI1 can repress target genes by recruiting HDAC1 and LSD1 corepressors to establish epigenetic silencing in other cell systems (20, 21), and their presence at *Runx2* is consistent with the multiple myeloma–induced decrease in activating marks H3K9ac and H3K4me3, respectively. Of note, LSD1 primarily acts on H3K4me1/2 substrates (42), but its presence regulating the H3K4 methylation state is primarily associated with gene repression and decreased levels of H3K4me3 at promoters (43). We made the novel observation that Gfi1 mediates the recruitment of EZH2 to *Runx2*, facilitating deposition of H3K27me3 at the *Runx2* promoter. Snail1, another member of the SNAG family of zinc finger transcription repressors (44), has also been

implicated in recruiting components of PRC2 during the repression of the *E-cadherin* (CDH1) gene in tumor cells (45) via the N-terminal repressor SNAG domain.

Studies with MC4 with a stable *Gfi1* knockdown demonstrated that lack of GFI1 binding to the *Runx2* promoter in multiple myeloma–exposed pre-osteoblast caused diminished recruitment of both HDAC1 and EZH2, preventing multiple myeloma–induced H3K9ac loss and H3K27me3 increase on *Runx2*. These changes allowed osteoblast differentiation, as evidenced by increased expression of *Runx2 and* the osteoblast differentiation markers *Ocn* and *Bsp*. Interestingly, *Gfi1* knockdown did not prevent the early multiple myeloma–induced decrease of *Runx2* mRNA. This indicates that destabilization of the *Runx2* mRNA is not sufficient to repress osteoblast differentiation and that GFI1-mediated chromatin changes are necessary for the multiple myeloma alteration of pre-osteoblast fate.

Several studies indicate that both HDAC1 and EZH2 are associated with negative regulation of osteoblastogenesis. Human mesenchymal stem cells exhibited increased osteogenic differentiation due to CDK1-dependent phosphorylation of EZH2, thereby causing disruption of PRC2 complex formation on *Runx2* and osteoblast-related gene promoters (46). Dudakovic and colleagues (47) reported that human stromal cells from the vascular fraction of adipose tissue displayed enhanced osteoblast differentiation if treated with EZH2 inhibitor or shRNA. Similarly, downregulation of HDAC1 activity was shown to promote osteoblast differentiation due to hyperacetylation of osteogenic gene promoters (48). Using the selective inhibitors MC1294 (HDAC1i) and GSK126 (EZH2i) to treat MC4 cells placed into osteoblast differentiation media after 72-hour multiple myeloma exposure, we demonstrated that blockade of either of these epigenetic modifiers rescued expression of *Runx2* as well as its downstream target osteoblast genes *Ocn*, *Bsp*, and *Alpl* from multiple myeloma–triggered repression. HDAC1 and EZH2 have a plethora of roles during osteoblast differentiation, and we observed that the universal targeting of these enzymes was slightly repressive on *Bsp* and *Alpl* expression in normal osteoblast differentiation samples. Despite this effect, the inhibitors had profound positive effects on the expression of these genes during osteoblast differentiation after multiple myeloma exposure. Furthermore, we reported that siRNA knockdown of *Gfi1* in BMSCs isolated from patients with multiple myeloma or after multiple myeloma exposure of MC4 cells also rescued the expression of these genes during induction of osteoblast differentiation (6). These results suggest that the multiple myeloma–induced epigenetic suppression of the *Runx2* promoter is a very dynamic and reversible process that requires continuous maintenance by GFI1 and its recruited repressive chromatin modifiers to prevent *Runx2* activation by stimulators of osteoblast differentiation. How GFI1 remains elevated in MM-BMSCs in the absence of multiple myeloma cells remains to be determined.

Here we provide evidence that suppression of the transition of BMSCs to functioning osteoblast in the proinflammatory myeloma bone marrow microenvironment is likely due to Gfi1-mediated and maintained epigenetic repression of the key osteoblast differentiation factor *Runx2* via recruitment of HDAC1 and EZH2. Interfering either with *Gfi1* expression or with HDAC1 or EZH2 activity reverses the epigenetic repression and permits osteoblast differentiation. These results suggest that treatment of patients with multiple myeloma with clinically available HDAC1 or EZH2 inhibitors may block or reverse the profound osteoblast suppression in multiple myeloma and allow repair of lytic lesions. Understanding the mechanisms associated with the repressive effects of GFI1 in BMSC may also lead to the development of novel therapeutics for MMBD as well as various inflammatory diseases such as rheumatoid arthritis that cause homeostatic imbalance in the bone microenvironment.

Disclosure of Potential Conflicts of Interest

R. Silbermann reports receiving a commercial research grant from American Cancer Society Institutional Research Grant. G.D. Roodman is a consultant/advisory board member of Amgen. No potential conflicts of interest were disclosed by the other authors.

Disclaimer

The contents of this article are solely the responsibility of the authors and do not necessarily represent the official views of the NIAMS, NCI, NIH, the Department of Veterans Affairs, or the United States Government.

Authors' Contributions

Conception and design: J. Adamik, S. Jin, D.L. Galson
Development of methodology: J. Adamik, S. Jin, Q. Sun, P. Zhang, D.L. Galson
Acquisition of data (provided animals, acquired and managed patients, provided facilities, etc.): J. Adamik, S. Jin, Q. Sun, P. Zhang, K.R. Weiss, J.L. Anderson, R. Silbermann, G.D. Roodman
Analysis and interpretation of data (e.g., statistical analysis, biostatistics, computational analysis): J. Adamik, S. Jin, Q. Sun, R. Silbermann, G.D. Roodman, D.L. Galson
Writing, review, and/or revision of the manuscript: J. Adamik, S. Jin, K.R. Weiss, G.D. Roodman, D.L. Galson
Administrative, technical, or material support (i.e., reporting or organizing data, constructing databases): S. Jin, P. Zhang
Study supervision: D.L. Galson

Acknowledgments

The authors gratefully thank the UPCI Lentivirus Facility for the SCR and shGfi1 lentiviruses; and the Veterans Administration Pittsburgh Healthcare System, Research and Development for use of their facilities.

Grant Support

This work was supported by the NIH Grants (R01AR059679 to D.L. Galson and G.D. Roodman and K08CA177927 to K.R. Weiss), the Veterans Administration (Merit Review to G.D. Roodman), and the Sarcoma Foundation of America (K.R. Weiss). This project used the UPCI Lentiviral and FACS facilities that are supported in part by NIH Grant P30CA047904.

The costs of publication of this article were defrayed in part by the payment of page charges. This article must therefore be hereby marked *advertisement* in accordance with 18 U.S.C. Section 1734 solely to indicate this fact.

Received July 19, 2016; revised December 16, 2016; accepted December 21, 2016; published OnlineFirst January 23, 2017.

References

1. Roodman GD. Pathogenesis of myeloma bone disease. J Cell Biochem 2010;109:283–91.
2. Saad F, Lipton A, Cook R, Chen YM, Smith M, Coleman R. Pathologic fractures correlate with reduced survival in patients with malignant bone disease. Cancer 2007;110:1860–7.
3. Sonmez M, Akagun T, Topbas M, Cobanoglu U, Sonmez B, Yilmaz M, et al. Effect of pathologic fractures on survival in multiple myeloma patients: a case control study. J Exp Clin Cancer Res 2008;27:11.
4. Galson DL, Silbermann R, Roodman GD. Mechanisms of multiple myeloma bone disease. BoneKEy Rep 2012;1:135.

5. Giuliani N, Rizzoli V, Roodman GD. Multiple myeloma bone disease: pathophysiology of osteoblast inhibition. Blood 2006;108:3992–6.
6. D'Souza S, del Prete D, Jin S, Sun Q, Huston AJ, Kostov FE, et al. Gfi1 expressed in bone marrow stromal cells is a novel osteoblast suppressor in patients with multiple myeloma bone disease. Blood 2011;118:6871–80.
7. Accardi F, Toscani D, Bolzoni M, Dalla Palma B, Aversa F, Giuliani N. Mechanism of action of bortezomib and the new proteasome inhibitors on myeloma cells and the bone microenvironment: impact on myeloma-induced alterations of bone remodeling. BioMed Res Int 2015;2015: 172458.
8. Arnulf B, Lecourt S, Soulier J, Ternaux B, Lacassagne MN, Crinquette A, et al. Phenotypic and functional characterization of bone marrow mesenchymal stem cells derived from patients with multiple myeloma. Leukemia 2007;21:158–63.
9. Corre J, Mahtouk K, Attal M, Gadelorge M, Huynh A, Fleury-Cappellesso S, et al. Bone marrow mesenchymal stem cells are abnormal in multiple myeloma. Leukemia 2007;21:1079–88.
10. Garderet L, Mazurier C, Chapel A, Ernou I, Boutin L, Holy X, et al. Mesenchymal stem cell abnormalities in patients with multiple myeloma. Leuk Lymphoma 2007;48:2032–41.
11. Hiruma Y, Honjo T, Jelinek DF, Windle JJ, Shin J, Roodman GD, et al. Increased signaling through p62 in the marrow microenvironment increases myeloma cell growth and osteoclast formation. Blood 2009;113: 4894–902.
12. Xu G, Liu K, Anderson J, Patrene K, Lentzsch S, Roodman GD, et al. Expression of XBP1s in bone marrow stromal cells is critical for myeloma cell growth and osteoclast formation. Blood 2012;119:4205–14.
13. Kobayashi T, Kronenberg H. Minireview: transcriptional regulation in development of bone. Endocrinology 2005;146:1012–7.
14. Giuliani N, Colla S, Morandi F, Lazzaretti M, Sala R, Bonomini S, et al. Myeloma cells block RUNX2/CBFA1 activity in human bone marrow osteoblast progenitors and inhibit osteoblast formation and differentiation. Blood 2005;106:2472–83.
15. Grimes HL, Gilks CB, Chan TO, Porter S, Tsichlis PN. The Gfi-1 proto-oncoprotein represses Bax expression and inhibits T-cell death. Proc Natl Acad Sci U S A 1996;93:14569–73.
16. Tateno M, Fukunishi Y, Komatsu S, Okazaki Y, Kawai J, Shibata K, et al. Identification of a novel member of the snail/Gfi-1 repressor family, mlt 1, which is methylated and silenced in liver tumors of SV40 T antigen transgenic mice. Cancer Res 2001;61:1144–53.
17. van der Meer LT, Jansen JH, van der Reijden BA. Gfi1 and Gfi1b: key regulators of hematopoiesis. Leukemia 2010;24:1834–43.
18. Fiolka K, Hertzano R, Vassen L, Zeng H, Hermesh O, Avraham KB, et al. Gfi1 and Gfi1b act equivalently in haematopoiesis, but have distinct, non-overlapping functions in inner ear development. EMBO Rep 2006;7:326–33.
19. Zweidler-Mckay PA, Grimes HL, Flubacher MM, Tsichlis PN. Gfi-1 encodes a nuclear zinc finger protein that binds DNA and functions as a transcriptional repressor. Mol Cell Biol 1996;16:4024–34.
20. Saleque S, Kim J, Rooke HM, Orkin SH. Epigenetic regulation of hematopoietic differentiation by Gfi-1 and Gfi-1b is mediated by the cofactors CoREST and LSD1. Mol Cell 2007;27:562–72.
21. Duan Z, Zarebski A, Montoya-Durango D, Grimes HL, Horwitz M. Gfi1 coordinates epigenetic repression of p21Cip/WAF1 by recruitment of histone lysine methyltransferase G9a and histone deacetylase 1. Mol Cell Biol 2005;25:10338–51.
22. Liu Q, Basu S, Qiu Y, Tang F, Dong F. A role of Miz-1 in Gfi-1-mediated transcriptional repression of CDKN1A. Oncogene 2010;29:2843–52.
23. Sharif-Askari E, Vassen L, Kosan C, Khandanpour C, Gaudreau MC, Heyd F, et al. Zinc finger protein Gfi1 controls the endotoxin-mediated Toll-like receptor inflammatory response by antagonizing NF-kappaB p65. Mol Cell Biol 2010;30:3929–42.
24. Dahl R, Iyer SR, Owens KS, Cuylear DD, Simon MC. The transcriptional repressor GFI-1 antagonizes PU.1 activity through protein-protein interaction. J Biol Chem 2007;282:6473–83.
25. Rodel B, Tavassoli K, Karsunky H, Schmidt T, Bachmann M, Schaper F, et al. The zinc finger protein Gfi-1 can enhance STAT3 signaling by interacting with the STAT3 inhibitor PIAS3. EMBO J 2000;19:5845–55.
26. Heyd F, ten Dam G, Moroy T. Auxiliary splice factor U2AF26 and transcription factor Gfi1 cooperate directly in regulating CD45 alternative splicing. Nat Immunol 2006;7:859–67.
27. Xiao G, Cui Y, Ducy P, Karsenty G, Franceschi RT. Ascorbic acid-dependent activation of the osteocalcin promoter in MC3T3-E1 preosteoblasts: requirement for collagen matrix synthesis and the presence of an intact OSE2 sequence. Mol Endocrinol 1997;11: 1103–13.
28. Wang D, Christensen K, Chawla K, Xiao G, Krebsbach PH, Franceschi RT. Isolation and characterization of MC3T3-E1 preosteoblast subclones with distinct *in vitro* and *in vivo* differentiation/mineralization potential. J Bone Miner Res 1999;14:893–903.
29. Adamik J, Wang KZ, Unlu S, Su AJ, Tannahill GM, Galson DL, et al. Distinct mechanisms for induction and tolerance regulate the immediate early genes encoding interleukin 1beta and tumor necrosis factor alpha. PLoS One 2013;8:e70622.
30. Gilbert L, He X, Farmer P, Rubin J, Drissi H, van Wijnen AJ, et al. Expression of the osteoblast differentiation factor RUNX2 (Cbfa1/AML3/Pebp2alpha A) is inhibited by tumor necrosis factor-alpha. J Biol Chem 2002;277: 2695–701.
31. Henikoff S, Shilatifard A. Histone modification: cause or cog? Trends Genet 2011;27:389–96.
32. Hansen KH, Bracken AP, Pasini D, Dietrich N, Gehani SS, Monrad A, et al. A model for transmission of the H3K27me3 epigenetic mark. Nat Cell Biol 2008;10:1291–300.
33. Montoya-Durango DE, Velu CS, Kazanjian A, Rojas ME, Jay CM, Longmore GD, et al. Ajuba functions as a histone deacetylase-dependent co-repressor for autoregulation of the growth factor-independent-1 transcription factor. J Biol Chem 2008;283:32056–65.
34. Margueron R, Reinberg D. The Polycomb complex PRC2 and its mark in life. Nature 2011;469:343–9.
35. Zarebski A, Velu CS, Baktula AM, Bourdeau T, Horman SR, Basu S, et al. Mutations in growth factor independent-1 associated with human neutropenia block murine granulopoiesis through colony stimulating factor-1. Immunity 2008;28:370–80.
36. Lee S, Doddapaneni K, Hogue A, McGhee L, Meyers S, Wu Z. Solution structure of Gfi-1 zinc domain bound to consensus DNA. J Mol Biol 2010;397:1055–66.
37. McCarty AS, Kleiger G, Eisenberg D, Smale ST. Selective dimerization of a C2H2 zinc finger subfamily. Mol Cell 2003;11:459–70.
38. Venkatesh S, Workman JL. Histone exchange, chromatin structure and the regulation of transcription. Nat Rev Mol Cell Biol 2015;16:178–89.
39. Guenther MG, Levine SS, Boyer LA, Jaenisch R, Young RA. A chromatin landmark and transcription initiation at most promoters in human cells. Cell 2007;130:77–88.
40. Tai PW, Wu H, Gordon JA, Whitfield TW, Barutcu AR, van Wijnen AJ, et al. Epigenetic landscape during osteoblastogenesis defines a differentiation-dependent Runx2 promoter region. Gene 2014;550:1–9.
41. Yang D, Okamura H, Nakashima Y, Haneji T. Histone demethylase Jmjd3 regulates osteoblast differentiation via transcription factors Runx2 and osterix. J Biol Chem 2013;288:33530–41.
42. Shi Y, Lan F, Matson C, Mulligan P, Whetstine JR, Cole PA, et al. Histone demethylation mediated by the nuclear amine oxidase homolog LSD1. Cell 2004;119:941–53.
43. Zentner GE, Henikoff S. Regulation of nucleosome dynamics by histone modifications. Nat Struct Mol Biol 2013;20:259–66.
44. Chiang C, Ayyanathan K. Snail/Gfi-1 (SNAG) family zinc finger proteins in transcription regulation, chromatin dynamics, cell signaling, development, and disease. Cytokine Growth Factor Rev 2013;24: 123–31.
45. Herranz N, Pasini D, Diaz VM, Franci C, Gutierrez A, Dave N, et al. Polycomb complex 2 is required for E-cadherin repression by the Snail1 transcription factor. Mol Cell Biol 2008;28:4772–81.
46. Wei Y, Chen YH, Li LY, Lang J, Yeh SP, Shi B, et al. CDK1-dependent phosphorylation of EZH2 suppresses methylation of H3K27 and promotes osteogenic differentiation of human mesenchymal stem cells. Nat Cell Biol 2011;13:87–94.
47. Dudakovic A, Camilleri ET, Xu F, Riester SM, McGee-Lawrence ME, Bradley EW, et al. Epigenetic control of skeletal development by the histone methyltransferase Ezh2. J Biol Chem 2015;290: 27604–17.
48. Lee HW, Suh JH, Kim AY, Lee YS, Park SY, Kim JB. Histone deacetylase 1-mediated histone modification regulates osteoblast differentiation. Mol Endocrinol 2006;20:2432–43.